

Reaction of Various Reductants with Oxide Films on Pt Electrodes As Studied by the Surface Interrogation Mode of Scanning Electrochemical Microscopy (SI-SECM): Possible Validity of a Marcus Relationship

Joaquín Rodríguez-López,[†] Alessandro Minguzzi,[‡] and Allen J. Bard^{*,†}

Center for Electrochemistry, Department of Chemistry and Biochemistry, University of Texas at Austin, 1 University Station A5300, Austin, Texas 78712-0165, United States, and Università degli Studi di Milano—Dipartimento di Chimica Fisica ed Elettrochimica, Via Golgi, 19, 20133, Milan, Italy

Received: August 2, 2010; Revised Manuscript Received: September 15, 2010

The surface interrogation mode of scanning electrochemical microscopy (SI-SECM), an in situ method for the quantification of adsorbed intermediates at electrodes at open circuit, was used to evaluate the rate of reaction of four redox mediators of different reducing power (methyl viologen⁺ > Ru(NH₃)₆²⁺ > Fe(II)[EDTA]²⁻ > Fe(CN)₆⁴⁻) with electrogenerated platinum oxides (PtO_x) at different pHs. The rate constant determined by SI-SECM was sensitive to the nature of the Pt oxide formed at different potentials. A simplified model with finite element method simulation was used to fit the SI-SECM experimental response. The extraction of kinetic constants and their comparison to the potential (reducing power) of the mediator yielded a Marcus-theory type relationship. Although these are clearly not outer sphere reactions, if subjected to the Marcus theory treatment, one can extract an estimated value of $\lambda = 1.3 \pm 0.3$ eV for the reduction of “place exchanged” oxide, which forms with oxide coverage values larger than 0.5 (as PtO). Steady state feedback experiments were also conducted in which the reduced form of the mediators was oxidized at Pt with different oxide coverage, i.e., over a wide range of potentials. A comparison of SI-SECM kinetic analysis with the Pt substrate at open circuit to the case where an electrode bias is applied indicates that for Fe(II)[EDTA]²⁻, the feedback current follows the oxide coverage at the Pt substrate. We suggest that thin layers of oxide provide a chemical route in which the oxide mediates oxidation of the reduced electrogenerated species; this route is governed by the reactivity of the different species of oxide formed at the electrode and not necessarily by other effects, such as direct electron tunneling through the oxide layer.

1. Introduction

The effect of electrode surface oxidation on the rate of apparently outer sphere electrode reactions (e.g., $R \rightarrow O + n\bar{e}$) has long been of interest. In such cases, at least two routes are possible: (1) reaction of the oxide directly with R and (2) tunneling of electrons from R through the oxide. It is difficult to address this problem with the usual electrochemical methods, but we show here that surface interrogation scanning electrochemical microscopy (SI-SECM)^{1–3} can be readily used for such studies. In particular, we discuss the determination of the chemical rate constants of reaction for a reduced form of a redox mediator (methyl viologen⁺, Ru(NH₃)₆²⁺, Fe(II)[EDTA]²⁻ and Fe(CN)₆⁴⁻) with Pt oxides formed under mildly anodic conditions (e.g., < 1.5 monolayers of “adsorbed O” as PtO). We further correlate the rate constants obtained with the energetics of the reaction and show that this path can be the predominant one for oxidation. The feedback mode of SECM, operating at steady state, can be used for measuring the kinetics of chemical and electrochemical processes. An SECM tip, which consists of an ultramicroelectrode (UME), interrogates a substrate at μm distances and is usually used to measure a steady-state current produced by the electrolysis of a redox mediator present in

solution. When the UME is close, this current is a function of the activity of the substrate.^{4,5} SI-SECM uses transient feedback as a means of measuring the amounts and kinetics of adsorbed reactants on the electrodes. In this study we use both steady-state and transient SECM measurements to evaluate the reactivity of Pt oxides.

Figure 1 is a schematic diagram of the methodology used in this study for a typical system in which an SECM tip with a metallic disk of radius $a = 12.5 \mu\text{m}$ ($\text{RG} \approx 2-3$, where $\text{RG} = \text{rg}/a$ and rg is the length of the flat end of the tip) is aligned to a substrate with radius $b = 25 \mu\text{m}$ at a distance $d < 3 \mu\text{m}$; Figure 1(A) depicts the kinetic characterization of the reaction of chemisorbed oxygen at the Pt substrate with an electrogenerated, reactive mediator produced at an SECM tip. As described earlier,¹ the first step for the implementation of SI-SECM consists of the generation of a limited amount of oxide at the Pt substrate, which is followed by the opening of the circuit for this electrode. This operation allows the study of the chemical reactivity of the formed oxide by the SECM tip; in this case, the tip generates a reducing agent R , from a species O in solution. This electrochemical reaction produces a measurable current at the tip. R diffuses to the substrate and reacts with the oxide, eq 1 for PtO (a $2\bar{e}$ process), thus regenerating O , which increases the flux of this species to the tip and in turn, transiently produces a larger current. This feedback cycle continues until all of the Pt oxide is consumed and the current at the tip decays to a background level. If the titrant R is generated in a linear potential sweep across the appropriate

* To whom correspondence should be addressed. E-mail: ajbard@mail.utexas.edu.

[†] Center for Electrochemistry, Department of Chemistry and Biochemistry, University of Texas at Austin.

[‡] Università degli Studi di Milano—Dipartimento di Chimica Fisica ed Elettrochimica.

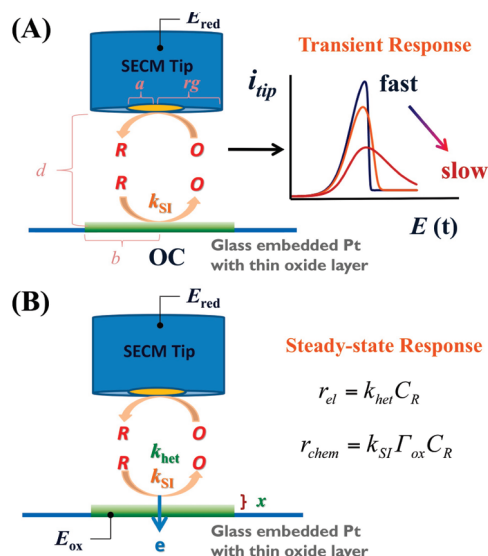


Figure 1. Schematic diagram (not to scale) of the system used to study oxide reactivity by transient and steady state feedback. (A) SI-SECM used to evaluate the open circuit chemical reactivity of Pt oxide. The tip “titrates” the oxide through a potential scan; sharper feedback curves indicate higher kinetics of reaction for the mediator with the oxide. (B) SECM in the feedback mode can be used to evaluate the steady state electron transfer across the oxidized Pt; two routes are possible: an electrochemical one with rate r_{el} , and a chemical one, with rate r_{chem} .

potential range for the O/R pair, then the response will be a curve similar to the ones shown schematically in Figure 1(A). The kinetics and mechanism of the reaction, characterized by an overall reaction constant k_{SI} , will determine the shape of the response curve; fast reactions will give sharp curves that decay quickly (E is a function of time) compared to slower ones. The mechanism and rate constants can then be obtained by comparison to digital simulation of this transient response. We demonstrate in this study how the kinetics of reaction change in response to differences in the driving force of the process, i.e. the reducing power of the mediator.



A great advantage of the SECM over other electrochemical techniques is that it allows decoupling of the analytical measurement from the operation of the substrate;⁴ this case is depicted in Figure 1(B). Here, the SECM tip generates the reduced species R at steady state while the substrate is biased to a potential at which it generates an oxide layer. At sufficiently positive potentials the substrate will regenerate O by oxidizing R , thus providing a feedback current at the tip.⁴ Changes in the kinetics of this oxidation reaction, which may be brought about by the formation of oxide, can be followed through measurement of the tip current, which is a reflection of how fast the substrate is feeding back oxidized mediator, O .^{6–8} Notice that the measurement of the oxidation rate is done in situ and at the desired potential of the substrate, in contrast to conventional single electrode measurements where the potential of the substrate would otherwise be changed to measure charge transfer kinetics of a redox mediator. By combining measurements done with the SI-SECM and feedback modes we propose that under certain conditions, the steady state substrate response can be described by a combination of chemical and electrochemical

routes (r_{chem} and r_{el} respectively in Figure 1(B)) for the oxidation of R , rather than a purely electrochemical path. The measurement of chemical processes at steady state with the SECM has been exploited since the introduction of the technique;^{9–12} and integrated approaches exist for the determination of substrate kinetics for combined electrochemical and chemical systems such as self-assembled monolayers.^{13,14} Our approach uses information obtained through transient measurements to decouple the possible contributions of the chemical route from those of the electrochemical route, as depicted in Figure 1(B), in an electrocatalytic system.

A particularly interesting case in the study of the oxidation of species on oxide covered Pt electrodes is the observation that the electrochemical response for some processes, as evaluated from the heterogeneous rate constant for electron transfer, is decreased upon oxide formation.¹⁵ Thick oxide passive layers on valve metals are known to act as insulating barriers for electron transfer;^{16,17} the decrease in the rate constant due to such layers can often be modeled in general terms according to eq 2:

$$k_{het,eff} = k_{het}e^{-\beta x} \quad (2)$$

where $k_{het,eff}$ is the effective rate of electron transfer across the insulating layer of thickness x ; k_{het} is the constant for electron transfer in the absence of insulating layer and β is the tunneling constant (typically taken as $\sim 1.1 \text{ \AA}^{-1}$, although smaller values have also been reported).^{13,18} Pt oxides decrease the rate of inner-sphere electrochemical reactions, such as the oxidation of hydrogen or alcohols or the reduction of protons or oxygen,¹⁹ where competitive adsorption plays a major role in the reaction mechanism.^{20,21} In other processes, such as the oxygen evolution reaction (OER), the formation of these oxides is central to the mechanism of reaction, and determining the effect of adsorbed oxygen is clearly of interest.^{20–23} A limited number of reports exist on the effect of Pt oxides on outer-sphere reactions, e.g., the oxidation of Fe(II) and As(III)¹⁵ or Ce(III) and Mn(II) species,²⁴ or $\text{Fe}(\text{CN})_6^{4-}$,^{25,26} where the participation of chemisorbed oxygen on the reduction mechanism was proposed, although no direct study of it was made. Our initial observations on the reactivity of Pt and Au oxides through the SI-SECM technique,¹ where reaction of the oxide with an in situ electrogenerated redox mediator produces a transient feedback response, motivated us to explain further the impact of the Pt oxide reactivity on the shape of the obtained tip electrochemical responses. This information can be used to explain the decrease in reactivity observed with certain mediators, like $\text{Fe}(\text{II})\text{EDTA}^{2-}$, at different stages of oxide formation on Pt. In a larger context, the introduction of this in situ SECM methodology to long-standing topics in electrocatalysis such as the higher-valence oxide mediation of the OER in metal oxides (e.g., IrO_2 , RuO_2 , or Co_3O_4)^{27,28} would be especially useful; such in situ measurements are still being developed and combined with new and powerful methods of characterization.^{28,29} In this study, we thus provide a first example of the capabilities of SECM in this research area with a simpler system.

There is a large body of literature on adsorbed oxygen on Pt. Studies of the electrochemical reactivity of Pt oxides formed at different stages of anodization have been proposed based on the shape of the surface reduction response observed in cyclic voltammetry,^{30,31} where electrochemical irreversibility is observed after the initial formation of a reversible oxide. This irreversibility has been ascribed to the formation of a “place

exchanged" oxygen species, i.e., oxygen buried into the surface layers of Pt.^{32,33} The characterization of the structure of surface Pt oxides however is challenging and still not well understood, even at single crystal electrodes.²⁰ In fact, there is no general agreement on the type of species of which Pt oxide consists; early CV studies suggested that PtOH and place exchanged OHPt were the relevant species in the initial stages of oxide formation.³⁰ Other measurements done ex-situ such as XPS and Auger spectroscopy suggest the formation of anhydrous PtO in varying amounts.^{34,35} For example, electrochemical quartz microbalance studies claim that 0.5 monolayer (ML) of PtO (2 \bar{e} per equivalent) are formed rather than 1 ML of differently coordinated PtOH (1 \bar{e} per equivalent)³⁶ for the first monolayer.

In this work, we will focus on the <2 ML PtO, i.e., equivalent to <880 $\mu\text{C}/\text{cm}^2$, or to roughly 4 \times an adsorbed hydrogen ML, Q_{H} (210 $\mu\text{C}/\text{cm}^2$). Thus, we assign $\theta_{\text{OX}} = 1$ (1 ML) at $Q_{\text{OX}} = 2Q_{\text{H}}$ (formally PtO) and 2 ML ($\theta_{\text{OX}} = 2$ at $Q_{\text{OX}} = 4Q_{\text{H}}$) (formally PtO₂).³² CV studies have suggested that changes in the kinetics of reduction start when forming $\sim 200 \mu\text{C}/\text{cm}^2$ ($\theta_{\text{OX}} \approx 0.5$) (formally PtOH); these observations are also complemented by changes in ellipsometric parameters at that coverage.³⁰ LEED studies performed ex-situ have suggested that the place exchange process starts in the range 200–300 $\mu\text{C}/\text{cm}^2$.³⁷ In-situ X-ray techniques also revealed morphologic changes at specific coverage, although identification of the involved species (i.e., adsorbed oxygen or hydroxyl) is not possible; place exchange in this case is suggested to occur between 0.6 \bar{e}/Pt to 1.2 \bar{e}/Pt , afterward coexisting with further formation of oxide on top of this structure until the surface disorders and roughens beyond 1.7 \bar{e}/Pt .^{38,39} Alternative models for oxide formation (which make predictions about their limiting growth) have suggested that the unit cell for two monolayers of PtO has a limiting thickness of 0.534 nm,⁴⁰ before formation of an outer phase of hydrated Pt oxide at more positive potentials.⁴¹ We study here the changes in reactivity of oxide species formed at a Pt substrate with respect to different reactive redox mediators. We find that upon reaching $\theta_{\text{OX}} \approx 0.5$ chemical rate limitations and changes in reaction kinetics are observed, and are considered in the simulation model used to fit the SI-SECM response. Our previous use of the SI-SECM technique focused on *quantification* of adsorbed species; in this case, we explore the application of the method for the study of the *reactivity* of adsorbed species with electrogenerated reductants in solution.

2. Experimental Section

All solutions were prepared with deionized Milli-Q water. Chemicals used as received were: sulfuric acid (94%–98%) trace metal grade from Fisher Scientific (Canada) used to prepare 0.5 M H₂SO₄; sodium acetate trihydrate (NaC₂H₃O₂, Fisher Scientific, ACS reagent) and acetic acid glacial from Mallinckrodt (Paris, KY) used to prepare acetate buffer solution pH = 4; tribasic, dibasic and monobasic potassium phosphate "Baker Analyzed" from J.T. Baker (Phillipsbury, NJ) as well as *o*-phosphoric acid 85% from Fisher Scientific (Fair Lawn, NJ) used to prepare 0.1 M solutions of phosphate buffer at the desired pH. Mediator solutions of the indicated concentration were prepared with the following: methyl viologen (MV) perchlorate and hexammineruthenium(III) (Ruhex) perchlorate were prepared by metathesis of methyl viologen dichloride hydrate (98%) from Aldrich (Milwaukee, WI) or hexammineruthenium(III) chloride (Ru(NH₃)₆Cl₃, 99%) from Strem Chemicals (Newburyport, MA) in concentrated solutions of sodium perchlorate (NaClO₄, 99%) from Aldrich (Milwaukee, WI). Potassium ferricyanide (K₃Fe(CN)₆·3H₂O, ACS reagent) from Fisher

Scientific was used as received. A 1:1 complex of Fe³⁺ and EDTA (FeEDTA) was prepared by mixing a 10% molar excess of (ethylenedinitrilo)- tetraacetic acid, disodium salt dihydrate (Na₂H₂EDTA·2H₂O, ACS reagent) from Fisher Scientific with iron(III) perchlorate nonahydrate (99%, Fe(ClO₄)₃·9H₂O) from Aldrich.

2.1. Electrodes. Gold (99.99+%) 25 μm diameter wire and platinum (99.99%) 25 and 50 μm diameter wire from Goodfellow (Devon, PA) were used to fabricate the SECM electrodes by procedures described elsewhere;⁴ the tips used in this work had an $RG \approx 3$. All metallic electrodes were polished prior to use with alumina paste (0.3 μm) on microcloth pads (Buehler, Lake Bluff, IL), and sonicated for 5 min in water. Pt electrodes were further cycled between -0.1 and 1.2 V versus RHE in their respective buffer to a constant CV before adsorption measurements. Unless otherwise noted, all tip electrodes were Au and all substrate electrodes were Pt.

In all experiments, an Ag/AgCl (sat'd KCl) reference electrode was used (chloride leakage from the Ag/AgCl reference was prevented by the use of a 0.1 M sodium perchlorate 3% w/v agar salt bridge prepared with agar purified grade from Fisher Scientific (Fair Lawn, NJ) and sodium perchlorate). However, all potential measurements are reported either versus RHE or NHE. Comparison of results for SI-SECM and feedback experiments at different substrate potentials and pH was done by conversion of the potential vs NHE to that of RHE, where $E_{\text{RHE}} \approx E_{\text{NHE}} + 0.059 \text{ pH}$, as validated in the Supporting Information, Figure S1. SI-SECM mediator CV scans are essentially pH independent, and are given vs NHE throughout the text. A 0.5 mm diameter tungsten wire (Alfa Products, Danvers, MA) was used in all experiments as a counter electrode. All solutions used in the electrochemical cell were thoroughly bubbled with Ar prior to experimentation and were kept under a humidified argon blanket.

SECM and other electrochemical measurements were done with a CHI 920C SECM station bipotentiostat (CH Instruments, Austin, TX) equipped with software for the automatic programming of SI-SECM. In the SI-SECM scheme, the substrate is stepped or swept to a given potential and then the circuit is open; after a selected delay time, the tip was activated through a CV scan to electrogenerate the reactive mediator; the potential window and scan rate were chosen differently for each mediator. Feedback experiments were performed at constant height and by applying a constant potential to the tip at diffusion limited conditions for reduction of the mediator. The substrate was scanned slowly to from $\sim +200$ mV from the mediator reduction wave onset to the desired anodic potential limit, stopping for 70 s at desired potentials, where steady state conditions in the presence of oxide growth are attained. The positioning and alignment of the electrodes was done as described in previous SI-SECM communications;^{1,2} in short, the tip was approached to the substrate in the feedback mode and scans in *x*, *y*, and *z* directions were run to optimize the feedback current. Distances were estimated during the experiment by the use of positive feedback theory⁴ and then fine-tuned by the use of simulations; chosen distances were in the range 3 $\mu\text{m} > d > 2 \mu\text{m}$.

Oxide coverage was estimated by comparison of the charge required for reduction of the oxide either by SI-SECM¹ or by conventional CV measurements (integration of the surface reduction wave).^{30,33} These amounts were compared to the integration of the UPD hydrogen response obtained through a linear potential scan on the Pt substrate to 0.03 V vs RHE in either blank buffer or 0.5 M H₂SO₄. For the SI-SECM determination of oxides, the result from integration of the

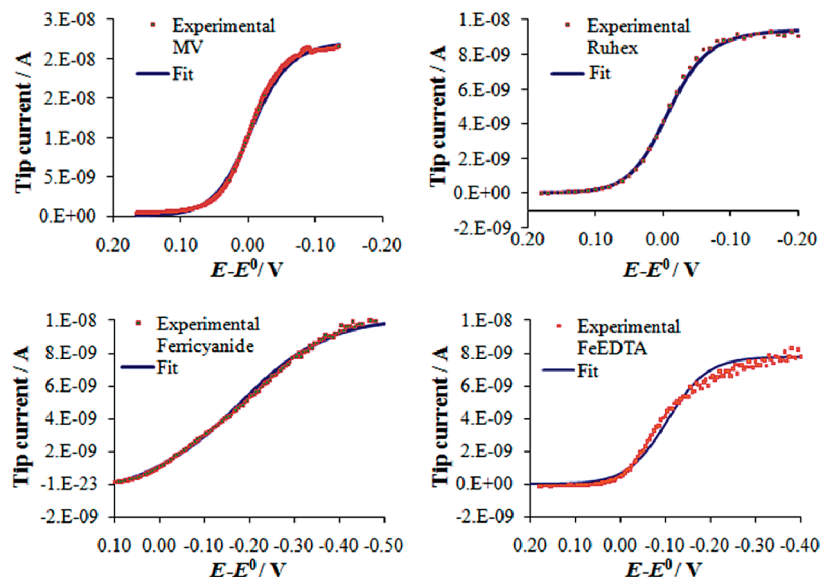


Figure 2. Determination of tip kinetic parameters for different mediators. Tip–substrate distance and obtained parameters are shown in Table 1. All determinations done on Au tip microelectrodes with radius $a = 12.5 \mu\text{m}$ with $RG \approx 3$; mediator used is indicated in each panel. Substrate for all measurements was Pt with radius $b = 25 \mu\text{m}$ and $RG \approx 3$. Substrate potentials as follows: MV, $E_{\text{sub}} = 0.7 \text{ V}$ vs RHE; Ruhex, $E_{\text{sub}} = 0.92 \text{ V}$ vs RHE; Ferricyanide, $E_{\text{sub}} = 1.22 \text{ V}$ vs RHE; FeEDTA, $E_{\text{sub}} = 1.12 \text{ V}$ vs RHE.

experimental background-subtracted scans was used as an initial guess in digital simulations. Because of the mismatch between the radius of the tip and that of the substrate, 100% recovery of the oxide is not predicted by the model; our simulations indicate that recovery was in the range of 80% to 85% (depending on k_{SI} and d and for $3 > RG > 2$ at the tip). This correction factor was taken into account for the oxide coverage and was validated through the simulation.

3. Simulations and Related Calculations

Different mediators will exhibit different electrochemical kinetics for the tip response; these differences are especially important under the increased mass transfer conditions encountered in the SECM operating conditions. The SI-SECM response is expected to be convoluted with the kinetics observed at the tip, i.e., complete positive feedback caused by a chemical reaction at the substrate should not differ in shape to that caused by electrochemical regeneration of the mediator. Therefore, the determination of the functional parameters for the simulation of the transient feedback response is in order. The relevant kinetic parameters for the simulation of SI-SECM scans were obtained through the use of eqs 3–6:⁴²

TABLE 1: Relevant Parameters for the Fitting of Positive Feedback CV Scans^a

mediator	d (μm)	E^0 (V vs NHE)	k^0 (cm s^{-1})	α	D (m^2s^{-1})
MV (pH = 11.3)	2.0	-0.45	2	0.5	7.2×10^{-10}
Ruhex (pH = 4, 2.1)	2.3	0.05	0.1	0.5	7.5×10^{-10}
Ruhex (pH = 6.8)	2.7	0.05	0.1	0.5	5.5×10^{-10}
FeEDTA (pH = 6.8)	2.6	0.12	2×10^{-3}	0.6	4.0×10^{-10}
ferricyanide (pH = 6.8)	2.1	0.4	5×10^{-3}	0.3	6.2×10^{-10}

^a All measurements done with a $12.5 \mu\text{m}$ Au UME and a $25 \mu\text{m}$ Pt UME substrate held at a potential where oxidation occurred under diffusion-limited conditions. E^0 values obtained from Ref.;⁴ reported value for ferricyanide is 0.36 V vs. NHE.

$$I_{\text{T}}(L, E) = \frac{0.68 + \frac{0.79377}{L} + 0.3315e^{-1.0672/L}}{\Theta + \frac{1}{k}} \quad (3)$$

$$\Theta = 1 + \frac{D_{\text{o}}}{D_{\text{R}}} e^{\left(\frac{nF}{RT}(E-E^0)\right)} \quad (4)$$

$$k = \frac{k^0 e^{-\alpha f(E-E^0)}}{m_{\text{o}}} \quad (5)$$

$$m_{\text{o}} = \frac{4D_{\text{o}}}{\pi a} \left(0.68 + \frac{0.78377}{L} + 0.3315e^{-1.0672/L} \right) \quad (6)$$

where the standard rate constant k^0 and the transfer coefficient α can be measured in terms of known quantities such as the distance, d (where $L = da$), the potential E and standard potential of reaction E^0 and the steady state tip current at infinite distance, $i_{\text{T},\infty}$; the experimental tip current can be compared by using the relation $i_{\text{T}} = I_{\text{T}}(L, E) \times i_{\text{T},\infty}$. The procedure to correct for the tip kinetics is especially important for the more sluggish electrochemical reactions (e.g., those for FeEDTA and ferricyanide) where considerable deviation from nernstian behavior is observed at the high mass transfer rates induced by the small electrode separation in the SECM.⁴³ Figure 2 shows the fit obtained for the experimental scans obtained for the four mediators used in this study, and Table 1 summarizes the used and obtained electrochemical parameters. MV and Ruhex show relatively uncomplicated kinetics, which is consistent with our previous results where a preliminary comparison to simulation did not necessarily require tip kinetics adjustments;¹ FeEDTA and ferricyanide show sluggish tip kinetics and correction for this was necessary.

Digital simulations of the coupled kinetic and diffusive problem required to describe the SI-SECM response were modeled with COMSOL Multiphysics software v3.2 for a 2D-axial symmetry coupled to a 1D symmetry representing the substrate electrode. The geometry of the simulation space was

adjusted for the experimental conditions of this study, where $a = 12.5 \mu\text{m}$, $b = 25 \mu\text{m}$ and for both electrodes $\text{RG} \approx 3$; the distance d was adjusted for each particular case. A detailed description and depiction of the simulation space and relevant boundary conditions is presented in the Supporting Information, including Figure S2.

In our first SI-SECM study of oxides on Au and Pt,¹ we observed that at larger substrate oxide coverage, typically after $\theta_{\text{OX}} = 0.5$ coverage, the kinetics of the chemical reaction between the mediator and oxygen became more sluggish, i.e., the rate constant appeared to decrease. Similarly, the observed response suggested more than one step in the reaction mechanism as observed from the presence of multiple waves consistent with a sequence of reactions.^{1,3} The surface interrogation process can be considered as analogous to an Eley–Rideal mechanism,⁴⁴ where a species in solution reacts with an adsorbed species at the substrate; the rate for this process can be written (eq 7, as also shown in Figure 1 panel B):

$$r_{\text{chem}} = k_{\text{SI}}\Gamma_{\text{ox}}C_{\text{R}} \quad (7)$$

where r_{chem} represents the rate of reaction derived from the chemical reaction (mol/s m^2) and C_{R} is the concentration of the reduced mediator at the surface of the substrate. Since in this mechanism the reducing agent is not adsorbed, the decrease in the rate of the process cannot be ascribed to competitive adsorption. Rather it can be described in terms of a decrease in the value of k_{SI} and/or the attainment of a limiting value in the simulated coverage Γ_{ox} .

In expressing the overall reaction rate of reduced mediator and oxide, there is probably a continuum of species that are a function of the potential and particular Pt electrode surface sites. We found here that these can be treated adequately by assuming discrete reactive oxide species and a two adjustable kinetic parameter fit. As explained in the introduction, the place exchange process is thought to take place at coverage values close to $\theta_{\text{OX}} = 0.5$ as observed by different techniques.^{30–39} The place exchange rearrangement implies that the accessible surface oxide is limited, thus we used the limiting value of $\Gamma_{\text{ox,max}} = Q_{\text{H}}/FA_{\text{sub}}$ to model the “front reactive oxide” 1 (nominally PtOH), which then leads to the formation of a second reactive oxide which is surface limited in the same amount, 2 (nominally PtO). As an example, consider the reaction modeling for these two types of oxide (e.g., a place exchanged oxide that gives rise to its precursor surface oxide upon reduction); the initial surface composition can then be expressed as in eq 8, the linking relationships between different types of oxides are shown in eqs 9 and 10, and the total rate of reaction is expressed in eq 11, which also serves to describe the changes in mediator surface concentration at the substrate.

$$\Gamma_{\text{ox},2} + \Gamma_{\text{ox},1} = \Gamma_{\text{ox,max}} \quad (8)$$

$$r_{\text{ox},2} = -k_2\Gamma_{\text{ox},2}C_{\text{R}} \quad (9)$$

$$r_{\text{ox},1} = -r_{\text{ox},2} - k_1\Gamma_{\text{ox},1}C_{\text{R}} \quad (10)$$

$$r_{\text{chem}} = r_{\text{O}} = -r_{\text{R}} = k_2\Gamma_{\text{ox},2}C_{\text{R}} + k_1\Gamma_{\text{ox},1}C_{\text{R}} \quad (11)$$

The proposed model is strongly drawn on assuming possible transformations such as that of PtO into PtOH, the latter being

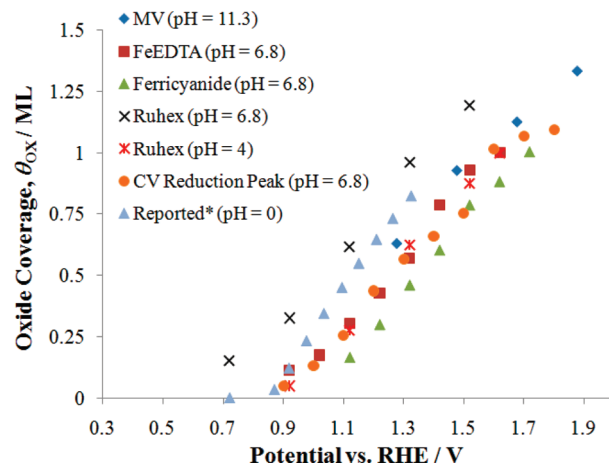


Figure 3. Estimated oxide coverage on Pt substrate in the presence of different mediators as a function of potential for oxidation of substrate. Coverage $\theta_{\text{OX}} = Q_{\text{OX}}/2Q_{\text{H}}$ where Q_{OX} is the charge of oxide determined by SI-SECM scans or CV on the oxide reduction peak and Q_{H} is the charge estimated by integration of the hydrogen adsorption area for the electrode in a mediator-free solution, $\theta_{\text{OX}} = 1$ implies 1 ML of equivalent PtO. Substrate in all cases is Pt with $b = 25 \mu\text{m}$, except labeled as CV Reduction Peak where a Pt electrode with $b = 12.5 \mu\text{m}$ was used. All values obtained after 70 s of oxidation at the indicated substrate potential. Reported* value in ref 33 0.5 M H_2SO_4 .

an intermediate state upon gaining an electron and a proton. The allowance that different oxide species involved have different reaction rate constants with respect to the reduced mediator is important in a description of the more complex tip response. As we show, we obtained reasonable fits to this model.

Steady state feedback simulations were also run in the same geometry used for the transient SI-SECM simulations, with the exception that an axial 2D problem suffices for this case and the substrate flux boundary condition shown in eq 12 is used to describe the rate of consumption of the reduced species:

$$r_{\text{R}} = -r_{\text{O}} = -k_{\text{het}}C_{\text{R}} \quad (12)$$

where C_{R} is again the concentration of the reduced species at the substrate and k_{het} the rate of heterogeneous electron transfer. Values for k_{het} were obtained for selected experiments with previous knowledge of the feedback current at the tip.^{4,6} The case where the oxide formed at a given potential at the substrate is responsible for sustaining the steady state feedback current through a chemical reaction with the mediator was also taken into account. The maximum feedback currents possible from the chemical route were calculated by transforming eq 12 into 13:

$$r_{\text{R}} = -r_{\text{O}} = -(k_n\Gamma_{\text{ox},n} + k_{n-1}\Gamma_{\text{ox},n-1})C_{\text{R}} \quad (13)$$

where n represents the higher order layer of front reactive oxide (e.g., if 2 layers, $n = 2$).

4. SI-SECM Reduction of Platinum Oxide at Open Circuit

The reduction of different amounts of Pt oxide at open circuit, obtained after bringing the Pt substrate to different potentials, was studied by performing SI-SECM with the different mediators introduced (MV, Ruhex, FeEDTA, and ferricyanide) and fitting the corresponding scans to the simulation model. Figure 3 shows the amounts of oxide formed at the selected potentials

TABLE 2: Coverage and Rate Parameters Used for the Fitting of SI-SECM Simulations to Experiment

mediator	$\Gamma_{\text{ox,max}}$ (nC) ^a	k_1 (m ³ mol ⁻¹ s ⁻¹)	k_2, k_3 (m ³ mol ⁻¹ s ⁻¹)
MV (pH = 11.3)	17	20	100
Ruhex (pH = 2.1)	20	20	100
Ruhex (pH = 4)	26	100	100
Ruhex (pH = 6.8)	20	10	30
FeEDTA (pH = 6.8)	20	10	6
ferricyanide (pH = 6.8)	15	0.75	2

^a In the simulation a molar surface concentration is used such that for a 25 μm radius substrate, with $A = 1.96 \times 10^{-9} \text{ m}^2$ each nC of total charge contributes $5.28 \times 10^{-6} \text{ mol m}^{-2}$.

obtained in the presence of the respective mediators in phosphate and acetate buffer and the comparison to the corresponding result in the absence of mediators, as well as the amounts reported in the literature for 0.5 M H_2SO_4 in ultrapure conditions.³³ Most of the oxide results obtained under the conditions of this study (e.g., in the presence of mediator and in buffer solution) follow the same roughly linear trend of coverage vs the potential of formation, so this same trend can be safely assumed to hold with the different mediators. The discrepancy between our oxide estimations and those reported in the literature may reside in the nature of the solution, e.g., the presence of the mediator itself in the medium could slightly affect the results, even if only very small amounts of the mediator adsorb onto the surface; the difference between the curves in the presence of mediator and those obtained by integration of the oxide reduction process in clean buffer is, however, small. The adsorption of phosphates or acetate may also cause a deviation; for example, the adsorption of anions has been reported to delay the appearance of the oxygen adsorption features, in the case of the weaker adsorption features by competitive adsorption or, in the case of place exchange by modifying electrostatically this field-assisted process.³¹ With the multicharged phosphates present in the buffers, electrostatic interactions may contribute significantly at positive potentials. However, most of our results fall within the same range of coverage vs potential, so we consider comparisons between the different systems to be valid. Ruhex at neutral pH shows some signs of side processes that prevent us from using this mediator for the steady state feedback experiments as explained in the Supporting Information (Figure S3), however, it presents the same reactivity trends as other mediators in SI-SECM experiments. Table 2 summarizes the results obtained for the fitting of the SI-SECM scans to the experiment. The maximum distinguishable rate constant for reaction of mediator with Pt oxide is $k_{\text{ST}} \approx 100 \text{ m}^3 \text{ mol}^{-1} \text{ s}^{-1}$, (different mediators were run at slightly different distances, d). The lowest measurable rate constant for the typical maximum coverage is $\sim 0.1 \text{ m}^3 \text{ mol}^{-1} \text{ s}^{-1}$. The accessible rate constants in this case cover the same 3-order of magnitude range observed for studies of heterogeneous electron transfer using steady state feedback at $L \approx 0.2$.^{4,6,8} The results presented in Table 2 show that the selection of mediators covered most of this range.

The results for the SI-SECM scans of MV at pH = 11.3 are shown in Figure 4 where increasing amounts of Pt oxide are titrated by electrogenerated MV^+ produced from the originally present MV^{2+} . MV^+ is a strongly reducing agent with a negative standard potential E^0 and very reactive toward O_2 reduction. We chose to use this mediator in basic solution since MV^+ also can participate in the direct pH-dependent reduction of H^+ to H_2 at the Pt surface.¹¹ SI-SECM scans were not possible at pH 6.8 due to high steady state backgrounds observed in blank measurements due to this process. At pH = 11.3, the background

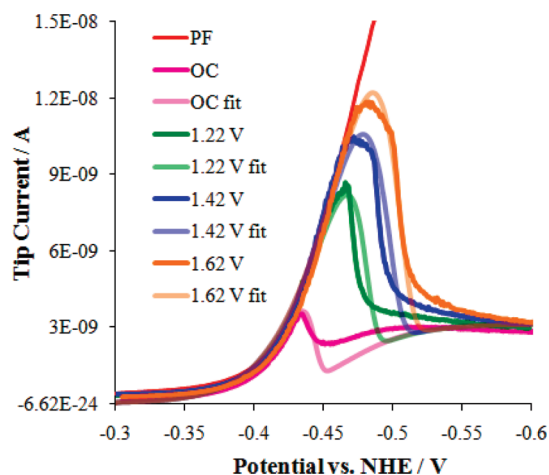


Figure 4. SI-SECM of Pt oxide using MV as mediator, pH = 11.3. Substrate held for 70 s at the indicated potential vs RHE in the label; Tip scan rate $\nu = 20 \text{ mV/s}$. $d = 2 \mu\text{m}$; background heterogeneous constant, $k_{\text{bkg}} = 3 \times 10^{-5} \text{ m/s}$. Solution is 1.1 mM in $\text{MV}(\text{ClO}_4)_2$ in 0.1 M phosphate buffer. Fitted rate constants: $k_1 = 20 \text{ m}^3 \text{ mol}^{-1} \text{ s}^{-1}$, $k_2 = 100 \text{ m}^3 \text{ mol}^{-1} \text{ s}^{-1}$.

levels were reasonable and the SI-SECM scans reveal the fast rate of the reaction of the mediator with the surface oxide species as shown by the sharp curves that follow the positive feedback (PF) scan and decay quickly after consuming most of the substrate adsorbate (Figure 4). Figure S4 (Supporting Information) confirms the fitting parameters by exploring the scan rate dependence of the SI-SECM signal; a good general agreement is observed in both cases across different amounts of oxide and different interrogation conditions with two fitting parameters (Table 2).

An important feature observed in Figure 4 and with most of the mediators in this work was the observation of a small distinguishable signal that appeared even in the background scans obtained when the substrate was interrogated after resting at open circuit (OC) for a long time in the presence of traces of air (that are difficult to avoid in the SECM cell, even with an Ar blanket), i.e., when the substrate was not purposely electrochemically oxidized. We have previously discussed these signals in terms of “incipient oxides” formed by chemical routes.¹ Reactive forms of oxygen species derived from adsorbed water have been suggested on Pt. For example, sum frequency generation spectra revealed the presence of OH stretch signals at $\text{pH} \approx 1$ that start at 0.4 V vs NHE, peak at 0.6 V and disappear beyond 0.9 V where the main Pt oxide starts to grow.⁴⁵ Activated oxygen species at potentials less positive than 0.9 V have been proposed in experimental and theoretical studies to be involved in processes such as the electrooxidation of carbon monoxide.^{46–48} Coverage by this incipient, or OC, oxygen depended on the pH as found in our experiments: pH = 4, $\theta_{\text{OX,OC}} \approx 0.025$ (Ruhex); pH = 6.8, $\theta_{\text{OX,OC}} \approx 0.15$ (Ruhex); pH = 6.8, $\theta_{\text{OX,OC}} \approx 0.06$ (FeEDTA); pH = 11.3, $\theta_{\text{OX,OC}} \approx 0.23$ (MV). The amount of these incipient oxides was previously reported to depend on pH and increase with increasing pH,⁴⁹ as observed here, although finding it by the SI-SECM technique also depends on the reducing power of the mediator used. Ferricyanide, the weakest reducing agent in this study, did not detect this type of oxide.

Note that the theoretical fits deviate slightly from the measured ones, especially during the final stages of the interrogation process as shown in Figure 4, i.e., experimental transients decayed less sharply than the simulated ones. This probably reflects effects of the diverse population of the

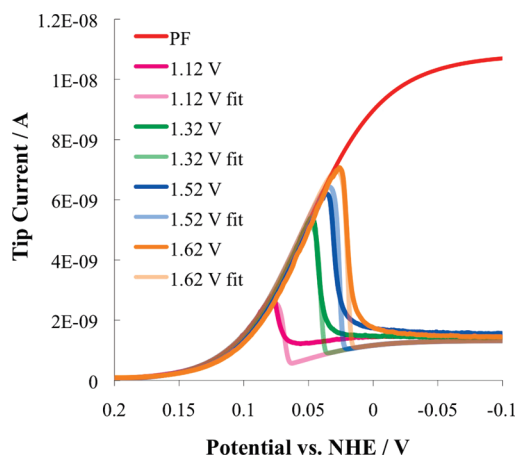


Figure 5. SI-SECM of Pt oxide using Ruhex as mediator, pH = 4. Substrate held for 70 s at the indicated potential vs RHE in the label; Tip scan rate $\nu = 10$ mV/s. $d = 2.3$ μm ; background heterogeneous constant, $k_{\text{back}} = 3 \times 10^{-5}$ m/s. Solution is 0.6 mM in $\text{Ru}(\text{NH}_3)_6(\text{ClO}_4)_3$ in 0.15 M acetate buffer. Fitted rate constants: $k_1 = 100$ $\text{m}^3 \text{mol}^{-1} \text{s}^{-1}$, $k_2 = 100$ $\text{m}^3 \text{mol}^{-1} \text{s}^{-1}$.

submonolayer species, e.g., PtOH with different configurations of OH, bridged to different numbers of Pt atoms depending on the coverage, where repulsive interactions between them could generate coverage dependent adsorption energies.^{20,30,39} These changes could result in a coverage dependent kinetic constant, where our model simply represents a constant k_1 as a first approximation. The formation of these species as a consequence of water activation over the metallic Pt surface would also imply that they are formed and consumed transiently near the end of the scan, a process that would inevitably generate tailing in our electrochemical signal. We note in this respect that we introduce k_1 values only as approximations; k_2 and k_3 values as will be shown, provide more interesting and reliable information about the kinetics of the oxide reduction process, especially in the case of higher (place exchanged) oxide.

The effects of the energetics of reaction of one mediator with the surface oxide can be tested by choosing a similar reducing agent. In Figure 5, we show the corresponding SI-SECM scans for Ruhex in acidic medium at pH = 4 (scans were also run and fit at pH = 2.1 with similar results). Provided that the E^0 of the mediator is not a pH sensitive process, the energetic gap between the mediator and the oxide can be increased by changing the pH of the solution (Figure S1 in the Supporting Information), since oxide reduction is pH dependent. Since $E^0 = 0.05$ V vs NHE for Ruhex, and is independent of pH, there is a higher free energy of reduction at lower pH; at pH = 4 in Figure 5 the SI-SECM scans reveal very sharp curves that denote fast interrogation kinetics, while Figure 6, which shows the interrogation results for Ruhex at pH = 6.8, show slower kinetics. In fact, upon reaching a substrate potential limit close to 1.32 V, there is a clear deviation of the scans from positive feedback. At this potential $\theta_{\text{OX}} > 0.5$, the reaction of higher oxide occurs and the decrease in kinetics can be ascribed to a decrease in the value of k_2 .

There is a similar effect when the mediator is FeEDTA ($E^0 = 0.12$ V vs NHE), and the rate of reaction of the oxide decreases further (Figure 7 and Supporting Information Figure S5 for low and high coverage of Pt oxide respectively, and where departure from the maximum rate of reaction set by the PF scans is evident). The measured kinetic constants for FeEDTA lie in the middle of the measurable range which is advantageous in terms of the goodness of the fit; in this range

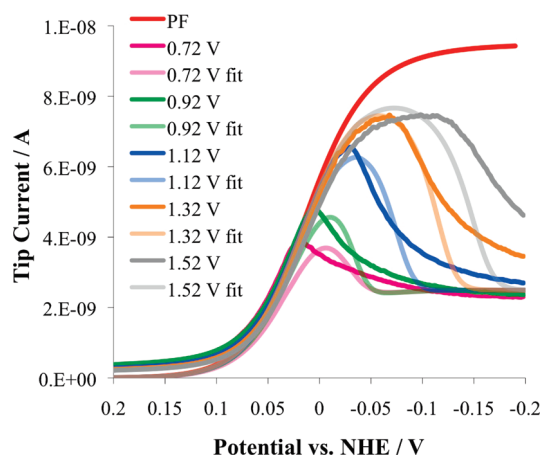


Figure 6. SI-SECM of Pt oxide using Ruhex as mediator, pH = 6.8. Substrate held for 70 s at the indicated potential vs RHE in the label; Tip scan rate $\nu = 20$ mV/s. $d = 2.7$ μm ; background heterogeneous constant, $k_{\text{back}} = 3 \times 10^{-5}$ m/s. Solution is 0.82 mM in $\text{Ru}(\text{NH}_3)_6(\text{ClO}_4)_3$ in 0.1 M phosphate buffer. Fitted rate constants: $k_1 = 10$ $\text{m}^3 \text{mol}^{-1} \text{s}^{-1}$, $k_2 = 30$ $\text{m}^3 \text{mol}^{-1} \text{s}^{-1}$.

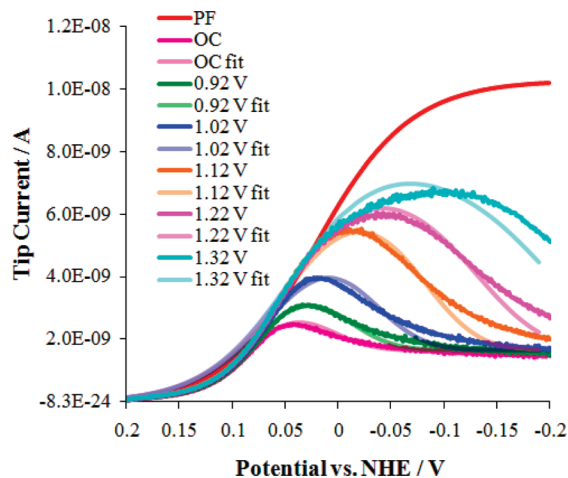


Figure 7. SI-SECM of Pt oxide using FeEDTA as mediator, pH = 6.8. Low coverage. Substrate held for 70 s at the indicated potential vs RHE in the label; Tip scan rate $\nu = 100$ mV/s. $d = 2.3$ μm ; background heterogeneous constant, $k_{\text{back}} = 1 \times 10^{-5}$ m/s. Solution is 0.89 mM in $\text{Fe}(\text{III})\text{EDTA}^-$ in 0.1 M phosphate buffer. Fitted rate constants: $k_1 = 10$ $\text{m}^3 \text{mol}^{-1} \text{s}^{-1}$, $k_2 = 6$ $\text{m}^3 \text{mol}^{-1} \text{s}^{-1}$.

subtle changes in k_1 and k_2 have a profound impact on the simulated shapes and thus, a better estimate of these can be given. Finally, Figure 8 shows the results for the least reducing mediator of the series, ferricyanide. The fit in this case revealed much smaller rate constants for the oxide reduction process. The rate is now so slow, compared to the full extent of positive feedback, as shown in the inset of Figure 8, that one might consider the system as nonreactive. However, the corresponding kinetic constants could be obtained within reasonable fits.

As shown in Tables 1 and 2, k_{SI} , depends on the driving force for reduction of the oxide (i.e., the free energy of the reaction between reductant and oxide). This free energy of reaction can be represented by the parameter ΔE , which equals the potential separation between the E^0 of the mediator and the peak potential of the electrochemical oxide reduction wave at $\theta_{\text{OX}} \approx 0.5$ at a given pH, as shown in Figure S1 (Supporting Information). A plot of the $\ln k_2$ vs ΔE (Figure 9) shows an approximately linear relationship. Homogeneous outer sphere reactions are often modeled by parabolic relationships with respect to the free energy of activation of the process in the context of Marcus

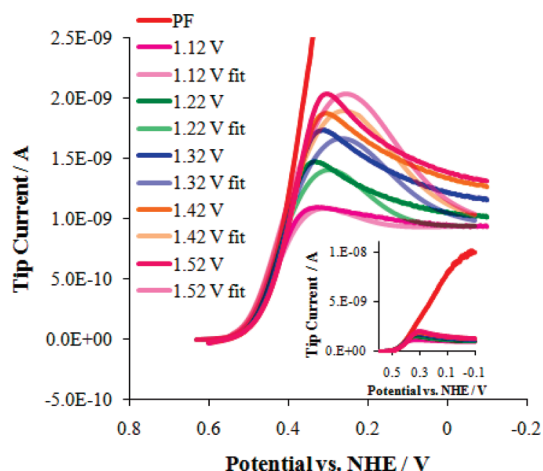


Figure 8. SI-SECM of Pt oxide using Ferricyanide as mediator, pH = 6.8. Substrate held for 70 s at the indicated potential vs RHE in the label; Tip scan rate $\nu = 20$ mV/s. $d = 2.1$ μm ; blank heterogeneous constant, $k_{\text{back}} = 1.1 \times 10^{-5}$ m/s. Solution is 0.65 mM in $\text{K}_3\text{Fe}(\text{CN})_6$ in 0.1 M phosphate buffer. Fitted rate constants: $k_1 = 0.75$ $\text{m}^3 \text{mol}^{-1} \text{s}^{-1}$, $k_2 = 2$ $\text{m}^3 \text{mol}^{-1} \text{s}^{-1}$. Inset shows full extent of PF scan for comparison to fitted curves.

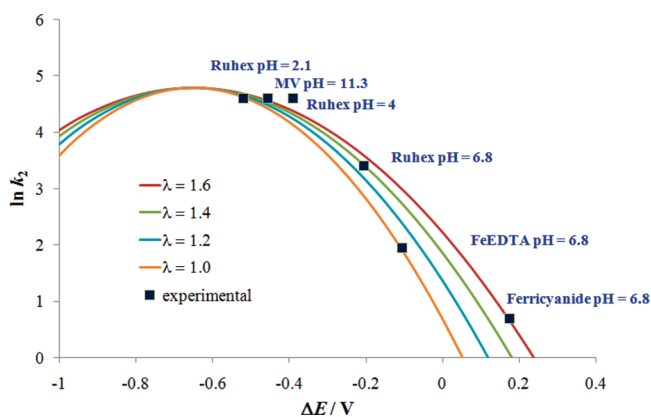


Figure 9. Dependence of the Pt oxide reduction rate constant on reducing power of mediator. ΔE stands for the difference between the E^0 of the mediator and the peak potential for electrochemical reduction of the oxide at the indicated pH. Values for k_2 as obtained from digital simulations in $\text{m}^3 \text{mol}^{-1} \text{s}^{-1}$. The graph also shows the parabolic curves obtained by use of eqs 14 and 15 with different values of λ/eV and adjusted to overlay on the data.

and related electron transfer theories,^{18,50–53} where the free energy of activation, ΔG^* , is expressed in terms of the driving force of the process ΔG^0 (in our case proportional to ΔE) and the reorganization energy, λ , e.g., the energy required to transform the nuclear configurations in the reactant and the solvent to those of the product state;¹⁸ eqs 14 and 15 are the relevant equations:^{18,52}

$$k_{\text{et}} = \frac{2\pi}{\hbar} |H_{\text{DA}}| \frac{1}{\sqrt{4\pi\lambda RT}} \exp\left(\frac{-\Delta G^*}{RT}\right) \quad (14)$$

$$\Delta G^* = \frac{F(\lambda + \Delta E)^2}{4\lambda} \quad (15)$$

where k_{et} is the rate constant for electron transfer, \hbar is the normalized Planck constant, $|H_{\text{DA}}|$ is the electronic coupling matrix element between the donor and acceptor states, R is the gas constant, and T the temperature;⁵² λ in this case is expressed

in eV. It is tempting to plot the data for the heterogeneous (inner sphere) reaction studied here to this formalism, and locate the calculated rate constants in the context of the parabolic relationship to obtain an estimate of λ ;⁵³ SECM kinetic measurements have been previously used to construct such parabolic relationships.⁵⁴ Such parabolas are shown in Figure 9 for values of λ ; our data would fall into the range $1.6 \text{ eV} > \lambda > 1.0 \text{ eV}$ so an average value of $\lambda = 1.3 \pm 0.3 \text{ eV}$ matches the rate constants fairly well. This value of λ is significantly larger than that attributable to the mediators and suggests that the reduction of the oxide, possibly the place-exchanged oxide (k_2 corresponds to the rate constant for reduction of $\theta_{\text{OX}} > 0.5$), is accompanied by a significant rearrangement of the products compared to the reactants. This is consistent with the model proposed by Nagy et al., in which considerable interactions, i.e., induced local fields, need to be overcome in order to reduce the place exchanged oxide,³⁸ and is also consistent with observations of loss of reversibility in cyclic voltammetry upon formation of the place exchanged oxide. The estimated λ value does not include corrections for work terms (e.g., Coulombic effects)¹⁸ that may be involved in eq 15, especially considering that the different mediators carry not only different charge, but also of opposite sign in some cases; nonetheless the agreement to the parabolic model is good. Larger (more negative) values of ΔE would be interesting so a possible inverted region could be examined, but could not be accessed due to the interference of parasitic catalytic processes at the Pt substrate.¹¹ However, less catalytically active surfaces, such as gold or mercury, may yield interesting results (although the generation of more reactive species in water starts to become a problem at potentials more negative than the ones used for MV).

5. Comparison of Chemical and Electrochemical Routes

We now turn to steady-state measurements of the oxidation of the mediator at the Pt substrate as a function of potential, particularly very positive (oxidizing) ones. Such measurements are difficult at a single electrode, but straightforward with the SECM, where generating a reducing redox mediator at the tip, while inducing strongly oxidizing conditions at the substrate with the formation of a reactive oxide can easily be accomplished. We can evaluate the impact of the formation of the oxide on Pt on the feedback and hence the rate of reaction (Figure 1(B)). Typically, SECM experiments of positive feedback do not involve bringing the substrate potential to extremely positive values, since for most well-behaved mediators, diffusion limited conditions of oxidation can be achieved within ~ 200 mV positive of the mediator E^0 . For example, in the case of MV feedback, with $E^0 = -0.45$ V vs NHE, the electrode needs not to be biased further than $E = -0.25$ V vs NHE to observe complete positive feedback; excursion into more positive potential regions where an oxide is formed is rarely carried out, although it is of interest in studying oxide film effects.

Figures 10 and 11 show the extremes of the chemical reactivity of a mediator with the Pt substrate under conditions of oxide formation with the tip set at a potential such that diffusion limited conditions apply, for MV (fast chemical kinetics with oxidized Pt) and for ferricyanide (slow chemical kinetics with oxidized Pt) respectively. In both cases, there is almost no change, within the standard deviation, in the feedback signal across potentials where Pt oxide forms. MV actually shows a very constant PF along a very wide range of potentials that only increases at the most positive potentials where O_2 evolution at the substrate can provide an additional contribution to the tip current (e.g., by collection of O_2 at Au or by

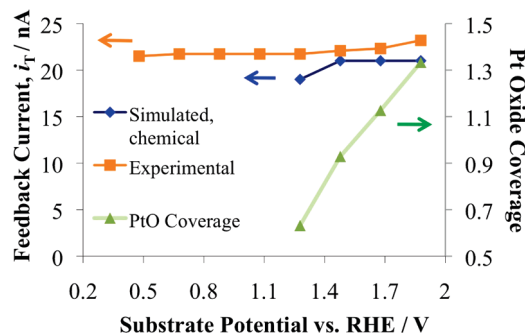


Figure 10. MV steady-state feedback on Pt at positive substrate potentials, at a fixed distance. $E_{\text{tip}} = -0.6$ V vs NHE; $d = 2 \mu\text{m}$ in 1.1 mM MV(ClO₄)₂ in pH = 11.3, 0.1 M Phosphate buffer. E_{sub} as indicated versus RHE; Pt oxide coverage as in Figure 3. All points recorded after first holding at the indicated substrate potential for 70 s and then maintaining the potential. Blue points indicate the simulated feedback response for the system if only the chemical route contributed to feedback.

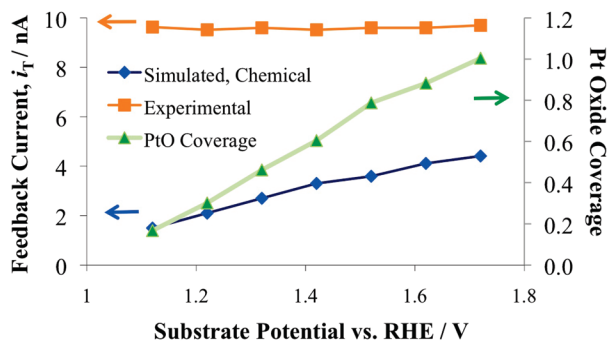


Figure 11. Ferricyanide feedback on Pt at anodizing substrate potentials, fixed distance. $E_{\text{tip}} = 0$ V vs NHE; $d = 2.1 \mu\text{m}$ in 0.65 mM K₃Fe(CN)₆ in pH = 6.8, 0.1 M Phosphate buffer. E_{sub} as indicated versus RHE; Pt oxide coverage as in Figure 3. All points recorded after first holding at the indicated substrate potential for 70 s and then maintaining the potential. Blue points indicate the simulated feedback response for the system if only the chemical route contributed to feedback.

homogeneous reaction with MV⁺). Under the conditions of this study, and considering the high chemical reaction constants found for MV with Pt oxides, the chemical route is indistinguishable from the electrochemical one, as shown by the simulated results in the presence of oxide at the Pt surface; in these, the rate of chemical reaction of the mediator in the presence of different amounts of oxide was the input. The replacement of the chemical rate, as obtained from the coverage of the different coexisting species with respect to the front reactive layer and their reaction kinetics, has been discussed in the simulation section. We assume that the composition of the surface oxide at steady state is the same as obtained from the initial state in the transient SI-SECM measurements. Similar results were obtained for Ruhex at pH = 2.1 and pH = 4 (not shown).

Similarly, the feedback of ferricyanide shows no change across potentials where oxide formation at the substrate is present. Feedback simulations are shown as well in Figure 11; here, the chemical feedback would only account for ~40% of the current at its maximum rate and no indication in either of these cases points to the predominance of the chemical route through the participation of the surface oxide in the feedback process; furthermore, no apparent loss of feedback activity is observed even when $\theta_{\text{OX}} \approx 1$.

Figure 12 shows the corresponding case for the feedback of FeEDTA at the oxide covered Pt substrate. Note that a previous

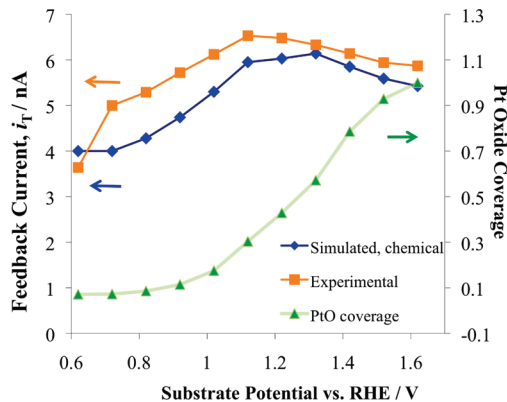


Figure 12. FeEDTA feedback on Pt at anodizing substrate potentials, fixed distance. $E_{\text{tip}} = -0.2$ V vs NHE; $d = 2.6 \mu\text{m}$ in 0.89 mM Fe(III)[EDTA]⁻ in pH = 6.8, 0.1 M Phosphate buffer. E^0 Fe(III)EDTA⁻ = 0.12 V vs NHE or a formal potential of 0.44 V vs RHE at pH 6.8. E_{sub} as indicated versus RHE; Pt oxide coverage as in Figure 3. All points recorded after first holding at the indicated substrate potential for 70 s and then maintaining the potential. Blue points indicate the simulated feedback response for the system if only the chemical route contributed to feedback.

study of FeEDTA electrochemistry on Pt has reported that it occurs by an EC mechanism producing a nonelectroactive intermediate and low collection at the ring at high rotation rates in rotating ring-disk electrode (RRDE) experiments.⁵⁵ In SECM experiments, we found the feedback response of FeEDTA to be sluggish at the less positive potentials and increased following a similar increase in the oxide coverage at the substrate. The feedback signal reached a maximum at a value of θ_{OX} larger than 0.3 and started decreasing at θ_{OX} slightly larger than 0.4, then kept decreasing until stabilizing at 1.62 V vs RHE (where $\theta_{\text{OX}} \approx 1$). Feedback simulations based on the coverage and reactivity with the oxide as the only means of Fe(II)EDTA²⁻ oxidation (Table 2) are also shown in Figure 12, and show a good agreement with the experimental data.

How does one explain the decrease in the rate of oxidation of Fe(II)EDTA²⁻ in the potential range 1.2 to 1.6 (potentials well positive of the formal potential of the species)? It cannot be explained by a Marcus inverted region for nonadiabatic electron transfer, since this is not found at metal electrodes; the thin Pt oxide film could be treated as a semiconductor with localized states, but for $\theta_{\text{OX}} \leq 1$ this is unlikely.¹⁶ For outer sphere reactions, tunneling effects, as suggested earlier in eq 2, on oxide-covered electrodes have been described. One could then ascribe the changes totally to electron transfer from the Fe(II)EDTA²⁻ as caused only by tunneling through the oxide film. Through feedback simulations, it is possible to extract the equivalent heterogeneous rate constant for the direct electron transfer through the oxide film, k_{het} , from the experimental feedback observed in Figure 12. A plot of the logarithm of this quantity versus the estimated thickness of the oxide can be made to assess the possibility of tunneling effects. Figure 13 shows such a plot, where the thickness of the Pt oxide was roughly estimated based on the density of bulk PtO;¹⁹ for $\theta_{\text{OX}} \approx 1$ this approach gives a reasonable estimate considering that two monolayers of Pt-O ($\theta_{\text{OX}} \approx 2$) have a thickness of 5.34 Å.⁴⁰ This plot shows good linearity, but the extracted value of the tunneling coefficient, $\beta = 0.33 \text{ \AA}^{-1}$ is small compared to the usual values,^{18,53} Tunneling effects have been typically reserved for thick layers of oxide on metals (e.g., thicker than 6 Å) while chemical effects are proposed to impact the rates of reaction on thinner ones.¹⁶

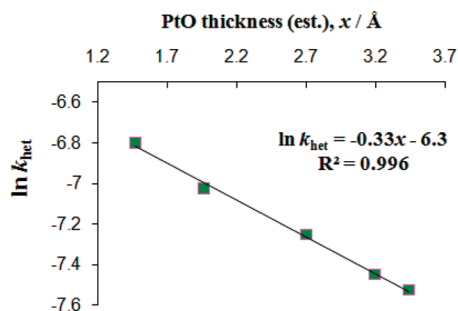


Figure 13. Logarithmic plot of heterogeneous substrate rate constant for FeEDTA feedback versus estimated PtO thickness. Points selected from Figure 12 in the substrate potential range 1.22–1.62 V vs RHE; increasing coverage implies increasing thickness. Values for the first order electrochemical rate constant k_{het} in m/s, calculated through digital simulation in the same conditions as obtained in Figure 12.

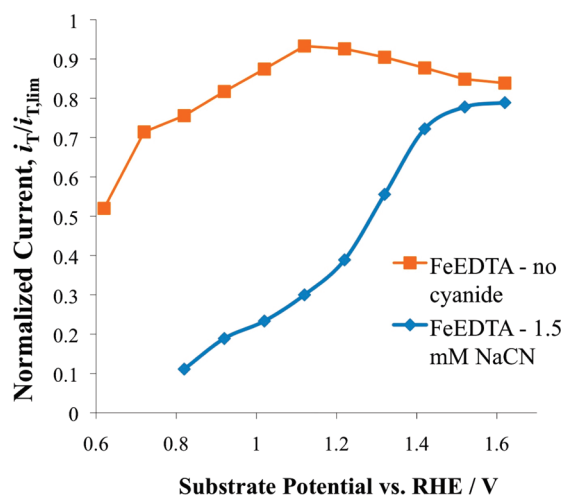


Figure 14. Effect of the addition of cyanide to FeEDTA feedback on Pt. $E_{\text{tip}} = -0.2$ V vs NHE; $d = 2.6$ μm for curve without cyanides (orange) and $d = 2.3$ μm for curve with cyanides (blue). Solution is 0.89 mM Fe(II)[EDTA] $^-$ in pH = 6.8, 0.1 M Phosphate buffer. E_{sub} as indicated versus RHE. $i_{T,\text{lim}}$ indicates average maximum feedback limit observed experimentally, curves are normalized to this value to correct for the different distance used.

Thus we prefer to explain the feedback behavior of FeEDTA in Figure 12 to the fact that oxidation occurs totally via reaction with the oxide, given the agreement between the simulated feedback from the SI-SECM model and the experimental response. To our knowledge, these chemical effects have not been addressed with the versatility that the SI-SECM technique allows. In this particular case, the oxidation of Fe(II)EDTA $^{2-}$ would be associated with the presence of oxide at the surface and its reactivity toward it, and the assumption that the higher oxides react more slowly. Notice also that these effects are observed well into the initial states of oxide formation, not only after reaching the first half monolayer of oxide. Since cyanide ion is known to inhibit oxide formation on Pt, 56 FeEDTA feedback experiments in the presence of cyanide ion, e.g., 1.5 mM NaCN were undertaken (Figure 14). Note the marked decrease in the feedback current in the oxide formation region (0.8 to 1.2 V vs RHE) until the cyanide adsorbate was stripped by oxidation from the surface at ~ 1.4 V vs RHE, where feedback was recovered. Cyanide adlayers are not expected to cause a significant tunneling effect, and in principle do not block all available sites at Pt, 57 although they drastically change inner-sphere processes. 58 This result strengthens our suggestion that there is a link between the formation of the reactive surface oxide and that of FeEDTA feedback, and that this relationship

is of a chemical nature. The addition of cyanides to the MV and ferricyanide systems had no impact on their feedback behavior.

These oxide effects are also relevant to inner sphere electrocatalytic processes that may be affected by coverage of oxide, e.g., when nonadsorbed reaction intermediates are reactive with the oxide. This includes complex reaction mechanisms, such as the oxygen reduction reaction, where oxidizable species, e.g., hydrogen peroxide, 21,59 might be released at potentials where submonolayers of oxide are present. Alcohol electrooxidations may also generate homogeneous species under similar conditions. 60 Although these are far more complex mechanisms than the reactions in this work, some electrocatalytic systems such as the oxidation of formic acid, 61 hydrogen 62 or hydrogen peroxide 63 may be treatable by the SI-SECM mode.

6. Conclusions

We have introduced the use of the surface interrogation mode of scanning electrochemical microscopy, SI-SECM, for the in situ determination of the kinetic parameters of the reaction of Pt oxides with redox mediators of different reducing power; measurements in the SI-SECM mode are performed at open circuit, so this allows us to obtain information about the chemical reactivity of these species through a versatile electrochemical setup. A simulation model that takes into account the formation of limiting surface amounts of oxides as well as their differential reactivity was used to fit the SI-SECM results obtained by the use of CV for the generation of the reducing species. Reasonable fittings were obtained across a space of different mediators, single and multiple-layered coverage values, scan rates, and pH. The kinetic constants for the reduction of the oxide formed at $\theta_{\text{OX}} > 0.5$ ($Q_{\text{OX}} > Q_{\text{H}}$), identified as the “place exchanged” oxide, were in agreement with the driving force of the process, which depended on the E^0 of the mediator and the pH. The results could be fitted successfully to a Marcus parabolic model, where only the forward side is observed; a value of the reorganization energy for the reduction of the oxide is estimated to be $\lambda = 1.3 \pm 0.3$ eV.

We further investigated the steady state reactivity of the oxide covered Pt substrate with the reduced mediators under conditions of electrochemical feedback. The electrochemistry of MV and ferricyanide oxidation appears not to be disturbed by the presence of the Pt oxide; however FeEDTA showed an initial increase in feedback signal followed by a decrease, which traces with changes in the oxide coverage and with the predicted chemical reactivity using the kinetic parameters obtained by SI-SECM. Our results suggest that changes in the electrochemistry of FeEDTA come as a consequence of its chemical reactivity with Pt oxides rather than on phenomena such as electron tunneling. Pt oxides are present in numerous electrocatalytic reactions, where the study of their reactivity with species in solution is of clear interest for the understanding of the mechanism of relevant reactions.

Acknowledgment. We thank the National Science Foundation (CHE-0808927) and the Robert A. Welch Foundation (F-0021) for support of this research. J.R.-L. thanks Eli Lilly & Company for a Division of Analytical Chemistry of the ACS fellowship; the complementary scholarship support provided by the Secretaria de Educacion Publica of Mexico and the Mexican Government is acknowledged. Financial support from the Ministry of Education, University and Research (PRIN 2008PF9TWZ) and Università degli Studi di Milano (PUR 2009 Funds, coordinator: Prof. S. Ardizzone) is gratefully acknowl-

edged. A.M. gratefully acknowledges the Università di Milano for a postdoc fellowship. The authors would also like to thank R. Cornut and C. Lefrou for their useful tips in COMSOL Multiscale modeling.

Supporting Information Available: The pH reversibility, simulation model. This information is available free of charge at <http://pubs.acs.org>. This material is available free of charge via the Internet at <http://pubs.acs.org>.

References and Notes

- Rodríguez-López, J.; Alpuche-Aviles, M. A.; Bard, A. J. *J. Am. Chem. Soc.* **2008**, *130*, 16985–16995.
- Rodríguez-López, J.; Bard, A. J. *J. Am. Chem. Soc.* **2010**, *132*, 5121–5129.
- Wang, Q.; Rodríguez-López, J.; Bard, A. J. *J. Am. Chem. Soc.* **2009**, *131*, 17046–17047.
- Scanning Electrochemical Microscopy*; Bard, A. J., Mirkin, M. V., Eds.; Marcel Dekker: New York, 2001. Also: Bard, A. J.; Fan, F.-R. F.; Mirkin, M. V. *Scanning Electrochemical Microscopy*. In *Electroanalytical Chemistry*; Bard, A. J., Ed.; Marcel Dekker: New York, 1993, Vol. 18, pp 243–373.
- Bard, A. J.; Denuault, G.; Lee, C.; Mandler, D.; Wipf, D. O. *Acc. Chem. Res.* **1990**, *23*, 357–363.
- Bard, A. J.; Mirkin, M. V.; Unwin, P. R.; Wipf, D. O. *J. Phys. Chem.* **1992**, *96*, 1861–1868.
- Wei, C.; Bard, A. J.; Mirkin, M. V. *J. Phys. Chem.* **1995**, *99*, 16033–16042.
- Cornut, R.; Lefrou, C. *J. Electroanal. Chem.* **2008**, *621*, 178–184.
- Mirkin, M. V.; Arca, M.; Bard, A. J. *J. Phys. Chem.* **1993**, *97*, 10790–10795.
- Macpherson, J. V.; Slevin, C. J.; Unwin, P. R. *J. Chem. Soc. Faraday Trans.* **1996**, *92*, 3799–3805.
- Selzer, Y.; Turyan, I.; Mandler, D. *J. Phys. Chem. B* **1999**, *103*, 1509–1517.
- For a comprehensive review on other cases: Pust, S. E.; Maier, W.; Wittstock, G. *Z. Phys. Chem.* **2008**, *222*, 1463–1517.
- Liu, B.; Bard, A. J.; Mirkin, M. V.; Creager, S. E. *J. Am. Chem. Soc.* **2004**, *126*, 1485–1492.
- Kiani, A.; Alpuche-Aviles, M. A.; Eggers, P. K.; Jones, M.; Gooding, J. J.; Paddon-Row, M. N.; Bard, A. J. *Langmuir* **2008**, *24*, 2841–2849.
- Baker, B. B.; MacNevin, W. M. *J. Am. Chem. Soc.* **1953**, *75*, 1476–1477.
- Schmickler, W.; Schultze, J. W. Electron Transfer Reactions on Oxide-Covered Metal Electrodes. In *Modern Aspects of Electrochemistry*; Bockris, J. O'M., Conway, B. E., White, R. E., Eds.; Plenum Press: New York, 1986. No. 17, 357–410.
- Moffat, T. P.; Yang, H.; Fan, F.-R. F.; Bard, A. J. *J. Electrochem. Soc.* **1992**, *139*, 3158–3167.
- Bard, A. J.; Faulkner, L. R. *Electrochemical Methods*; Wiley: New York, 2001.
- Schultze, J. W.; Vetter, K. *J. Electrochim. Acta* **1973**, *18*, 889–896.
- Markovic, N. M.; Ross, P. N., Jr. *Surf. Sci. Rep.* **2002**, *45*, 117–229.
- Fuel Cell Catalysis, A Surface Science Approach*; Koper, M. T. M., Ed.; John Wiley & Sons: Hoboken, NJ, 2009. (Andrzej Wieckowski, Series Ed.).
- Damjanovic, A.; Ward, A. T.; O'Jea, M. *J. Electrochem. Soc.* **1974**, *121*, 1186–1190.
- Damjanovic, A.; Birss, V. I.; Boudreaux, D. S. *J. Electrochem. Soc.* **1991**, *138*, 2549–2555.
- Kuhn, A. T.; Randle, T. H. *J. Chem. Soc. Faraday Trans. I* **1985**, *81*, 403–419.
- Kabanova, O. L. *Zh. Fiz. Khim.* **1961**, *35*, 2465–2471.
- Kabanova, O. L. *Zh. Anal. Khim.* **1961**, *16*, 135–140.
- Trasatti, S. *Electrochim. Acta* **1984**, *11*, 1503.
- Fierro, S.; Nagel, T.; Baltruschat, H.; Comminellis, C. *Electrochem. Commun.* **2007**, *9*, 1969.
- McAlpin, J. G.; Surendranath, Y.; Dinca, M.; Stich, T. A.; Stoian, S. A.; Casey, W. H.; Nocera, D. G.; Britt, R. D. *J. Am. Chem. Soc.* **2010**, *132*, 6882–6883.
- Angerstein-Kozłowska, H.; Conway, B. E. *J. Electroanal. Chem.* **1973**, *43*, 9–36.
- Angerstein-Kozłowska, H.; Conway, B. E.; Barnett, B.; Mozota, J. J. *Electroanal. Chem.* **1979**, *100*, 417–446.
- Tremilosi-Filho, G.; Jerkiewicz, G.; Conway, B. E. *Langmuir* **1992**, *8*, 658–667.
- Conway, B. E.; Angerstein-Kozłowska, H. *Acc. Chem. Res.* **1981**, *14*, 49–56.
- Dickinson, T.; Povey, A. F.; Sherwood, P. M. A. *J. Chem. Soc. Faraday Trans.* **1975**, *71*, 298–311.
- Wagner, F. T.; Ross, P. N., Jr. *App. Surf. Sci.* **1985**, *24*, 87–107.
- Jerkiewicz, G.; Vatankhah, G.; Lessard, J.; Soriaga, M. P.; Park, Y.-S. *Electrochim. Acta* **2004**, *49*, 1451–1459.
- Wagner, F. T.; Ross, P. N., Jr. *Surf. Sci.* **1985**, *160*, 305–330.
- Nagy, Z.; You, H. *Electrochim. Acta* **2002**, *47*, 3037–3055.
- You, H.; Zurawski, D. J.; Nagy, Z.; Yonco, R. M. *J. Chem. Phys.* **1994**, *100*, 4699–4702.
- Sun, A.; Franc, J.; Macdonald, D. D. *J. Electrochem. Soc.* **2006**, *153*, B260–B277.
- Xia, S. J.; Birss, V. I. *Electrochim. Acta* **1998**, *44*, 467–482.
- Mirkin, M. V.; Bard, A. J. *J. Anal. Chem.* **1992**, *64*, 2293–2302.
- Sun, P.; Mirkin, M. V. *Anal. Chem.* **2006**, *78*, 6526–6534.
- Atkins, P. W. *Processes at Solid Surfaces. Physical Chemistry*, 6th ed.; Oxford University Press: Oxford, 2000, pp 849–876.
- Noguchi, H.; Okada, T.; Uosaki, K. *Faraday Discuss.* **2008**, *140*, 125–137.
- Bergelin, M.; Feliu, J. M.; Wasberg, M. *Electrochim. Acta* **1998**, *44*, 1069–1075.
- Anderson, A. B.; Neshev, N. M.; Sidik, R. A.; Shiller, P. *Electrochim. Acta* **2002**, *47*, 2999–3008.
- Anderson, A. B. *Electrochim. Acta* **2002**, *47*, 3759–3763.
- Marichev, V. A. *Electrochem. Commun.* **2008**, *10*, 643–646.
- Andrieux, C. P.; Savéant, J.-M.; Su, K. B. *J. Phys. Chem.* **1986**, *90*, 3815–3823.
- Saveant, J.-M. *Elements of Molecular and Biomolecular Electrochemistry*; Wiley-Interscience: Hoboken, N.J., 2006.
- Fletcher, S. *J. Solid State Electrochem.* **2010**, *14*, 705–739.
- Miller, C. J. Heterogeneous Electron Transfer Kinetics at Metallic Electrodes. In *Physical Electrochemistry, Principles, Methods and Applications*; Rubinstein, I., Ed.; Marcel Dekker: New York, 1995, pp 27–79.
- Barker, A. L.; Unwin, P. R.; Amemiya, S.; Zhou, J.; Bard, A. J. *J. Phys. Chem. B* **1999**, *103*, 7260–7269.
- González, I.; Ibáñez, J. G.; Cárdenas, M. A.; Rojas-Hernández, A. *Electrochim. Acta* **1990**, *35*, 1325–1329.
- Huerta, F. J.; Morallon, E.; Vazquez, J. L.; Aldaz, A. *Surf. Sci.* **1998**, *396*, 400–410.
- Huerta, F.; Morallon, E.; Vazquez, J. L. *Electrochem. Commun.* **2002**, *4*, 251–254.
- Cuesta, A.; Escudero, M.; Lanova, B.; Baltruschat, H. *Langmuir* **2009**, *25*, 6500–6507.
- Sánchez-Sánchez, C. M.; Bard, A. J. *J. Anal. Chem.* **2009**, *81*, 8094–8100.
- Leiva, E.; Sánchez, C. Theoretical Aspects of Some Prototypical Fuel Cell Reactions. In *Handbook of Fuel Cells*; Vielstich, W., Lamm, A., Gasteiger, H., Eds.; Wiley: Chichester, England, 2003, Vol. 2, pp 93–131.
- Jung, C.; Sánchez-Sánchez, C. M.; Lin, C.-L.; Rodríguez-López, J.; Bard, A. J. *J. Anal. Chem.* **2009**, *81*, 7003–7008.
- Zhou, J.; Zu, Y.; Bard, A. J. *J. Electroanal. Chem.* **2000**, *491*, 22–29.
- Fernandez, J. L.; Hurth, C.; Bard, A. J. *J. Phys. Chem. B* **2005**, *109*, 9532–9539.